CrossMark

Investigation on a creep-tested CB2 steel cross-weld sample welded with a matching flux-cored wire

S. Baumgartner[1] · H. Pahr[1] · T. Zauchner[1]

Abstract

Heavy cast components like steam turbine or valve casings made of GX13CrMoCoVNbNB9-2-1 (CB2 steel) are used in modern fossil-fired power plants for service temperatures up to 620 °C. For production welding of these huge components, high productivity and good out-of-position weldability are needed. To combine these requirements, flux-cored arc welding is a preferred welding process. A matching flux-cored wire consumable has been developed, which offers sufficient short-term mechanical properties at ambient temperature. To prove weld metal long-term properties at service temperature, uniaxial creep rupture tests at 625 °C have been started several years ago. The microstructure of a cross-weld sample, ruptured in the heat-affected zone, was investigated by light optical microscopy and scanning electron microscopy with energy dispersive X-ray analyses. Area fraction and mean radius of precipitated Laves phase and $M_{23}C_6$ carbides were compared to the results of MatCalc™ simulations.

1 Introduction

The worldwide electricity consumption is assumed to increase by 2.1% per year up to 2040. Although, renewable energy sources will play a growing role, it is estimated that fossil fuels will continue to cover most of the demand [1]. Research programs in Europe, the USA, Japan and recently, in China and India as well have been performed to develop materials for advanced ultra-supercritical (A-USC) power plants with increased steam temperatures up to 700 °C and above, to increase the efficiency of thermal power plants and thereby reducing fuel consumption and CO_2 emission [2]. The European Cooperation in Science and Technology (COST) programs 501, 522 and 536, from 1983 to 2009, focused on the development of 9–12% Cr steels with increased creep strength. The B-alloyed 9Cr-1.5Mo-1Co cast steel CB2 showed the most promising creep strength, which is provided by finely dispersed MX carbonitrides and B-stabilized $M_{23}C_6$ carbides [3, 4]. The typical chemical composition is given in Table 1.

Long-term creep tests exceeding 130,000 h confirm the improved creep rupture strength of CB2 steel up to 650 °C, which has already been used for cast components such as turbine casings and valve bodies with operating temperatures up to 620 °C [5].

1.1 Welding of heavy cast components

Welding is an essential processing step in the production of heavy cast components. After non-destructive testing, all unacceptable indications are excavated and welded (process welding). Fabrication welding of weld-on components is carried out at once [6]. Due to economic aspects and the comparatively difficult handling of such huge components, high productivity combined with good out-of-position weldability is requested. Therefore, flux-cored arc welding (FCAW) is a preferred process.

1.2 Development of a matching flux-cored wire consumable

In parallel to the base material development, several consumable manufacturers started the design of matching

✉ S. Baumgartner
   susanne.baumgartner@voestalpine.com

[1] voestalpine Böhler Welding Austria GmbH, Kapfenberg, Austria

Table 1 Typical chemical analysis of CB2 base material (wt%) [5]

C	Mn	Cr	Mo	Co	V	Nb	N	B	Fe
0.14	0.3	9.5	1.5	1.25	0.2	0.05	0.02	0.01	Remainder

Table 3 Typical mechanical properties of all-weld metal acc. EN 15792-1 at ambient temperature with PWHT 730 °C/24 h

Yield strength	590 MPa
Tensile strength	740 MPa
Elongation	17%
The average Charpy V absorbed	30 J

consumables for shielded metal arc welding [7, 8]. As flux-cored wires (FCW) for gas metal arc welding are becoming more and more popular even in power generating industry, a matching FCW for welding CB2 steel was developed and classified as T ZCrMoCo9VNbNB P M 1 (EN ISO 17634-A). To ensure appropriate mechanical properties, a rutile-basic slag system was chosen.

The chemical composition of the all-weld metal was kept close to the chemical composition of the base material. The boron content had to be established carefully as boron is important to stabilize the microstructure, but shows a detrimental influence on hot cracking susceptibility and impact toughness [9]. Typical values of chemical composition and mechanical properties at ambient temperature for all-weld metal with post-weld heat treatment (PWHT) of 730 °C/24 h and air cooling, according to the product data sheet of Böhler CB 2 Ti-FD, are given in Tables 2 and 3, respectively [10].

To evaluate the long-term properties, creep rupture tests (CRT) at 625 °C for all-weld metal specimens and matching cross-weld samples were started several years ago. As creep tests are very expensive and time-consuming, they are intended to estimate the creep rupture strength by modelling in future. The first step, which is performed in this work, is to model the evolution of precipitates with the thermo-kinetic software package MatCalc™ depending on chemical composition and temperature cycle and to calculate phase fraction, mean radius and number density of the precipitates. To evaluate the model, the calculated values of Laves phase are compared to experimental results. Therefore, stereo optical microscopy (SOM), light optical microscopy (LOM) and scanning electron microscopy (SEM) investigations on fractured creep samples are carried out. The observed precipitates are characterized by energy dispersive X-ray spectra (EDX). Area fraction and precipitate size are statistically evaluated.

This contribution shows the status of creep rupture tests and compares the outcome of the simulation to the experimental results of microstructural investigation of a creep-tested cross-weld sample.

2 Experimental procedure

2.1 Joint preparation and welding parameters

The seam preparation and the schematic layer sequence of the welded joint are illustrated in Fig. 1a, b, respectively. The welding parameters are listed in Table 4. The welding procedure for all-weld metal tests is described in [11]. PWHT of 730 °C for 24 h with heating and cooling rate of 80 °C/h are performed on all-weld metal and the welded joint which represents the PWHT of large cast components with multiple welding cycles. Specimens for tensile tests, the Charpy V-notch tests and creep rupture tests were taken after PWHT.
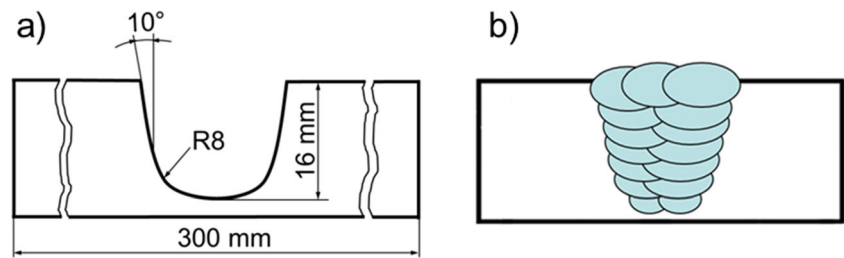
2.2 Creep rupture tests

Uniaxial CRT of all-weld metal and cross-weld samples were carried out at 625 °C with different loads.

2.3 Metallographic sample preparation

The metallographic samples were longitudinally wire cut (EDM), resin-mounted and prepared for SOM, LOM and SEM. The last polishing step was performed with 1 μm polycrystalline diamond suspension. Creep voids can better be observed in unetched condition. For LOM investigation, weld cross-sections were etched with Villela. To investigate the microstructure after CRT in

Table 2 Typical chemical composition of Böhler CB 2 Ti-FD flux-cored wire weld metal (wt%)

C	Si	Mn	Cr	Mo	Co	Ni	V	Nb	N	B	Fe
0.12	0.2	0.9	9.0	1.5	1.0	0.2	0.2	0.03	0.02	0.006	Remainder

Fig. 1 **a** Joint preparation. **b** Schematic layer sequence

detail, SEM and EDX analyses were performed subsequently after polishing with 0.2 μm silica oxide suspension. Pictures were taken in high resolution for further computer-based particle analyses.

2.4 Hardness measurements

A hardness profile according ISO 6507 was carried out on the cross-section of the creep-tested sample in polished condition.

2.5 Simulation of microstructural evolution

To estimate the evolution of precipitates in the weld metal during multi-pass welding, PWHT and service at 625 °C, calculations with the thermo-kinetic software package MatCalc™ were carried out. The typical chemical composition of all-weld metal given in Table 2 was used for the calculation with MatCalc version 6.00 and database_me_fe. To simulate the temperature effect of multi-pass welding, a temperature profile with subsequent peak temperatures of 1300, 1100 and 700 °C, respectively, was used. An interpass temperature of 250 °C and a cooling time of 20 s between 800 and 500 °C were applied for every cycle. The schematic temperature-time diagram is shown in Fig. 2. Phase

fraction, mean radius and number density of Cr-rich carbides (M_7C_3 and $M_{23}C_6$), MX precipitates (NbC and VN), BN and Laves phase were calculated. The precipitates were allowed to form at dislocations, grain boundaries and subgrain boundaries, respectively.

3 Results
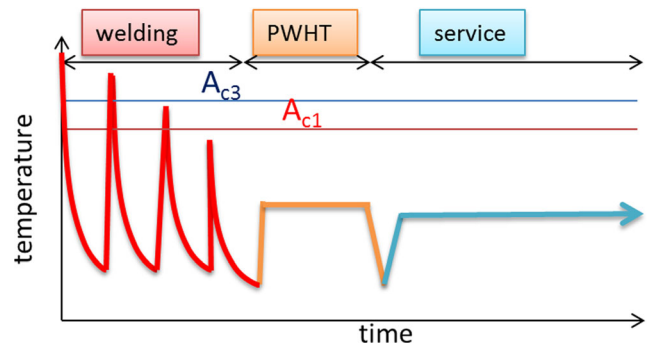
3.1 Short-term mechanical properties

Tensile tests at ambient temperature and hot tensile tests at 625 °C were performed on cross-weld and longitudinal weld metal specimens as well as the Charpy *V*-notch tests of the weld metal on cross-weld specimens. The results are listed in Table 5. Tensile strength (T.S.) of the longitudinal samples of the weld metal is higher than the result of the cross-weld samples which fractured in the heat-affected zone (HAZ) in both conditions.

3.2 Creep rupture tests

Uniaxial CRT of all-weld metal and cross-weld specimens were carried out at 625 °C with different loads. All ruptured specimens are within the − 20% median line of the COST CB2 trial melt base material as shown

Table 4 Welding parameters

|	
Base material	CB2 1742 B05
Position	PA (1G)
Shielding gas	Ar + 18%CO2
Preheat temperature	250 °C
Interpass temperature	260 °C
Wire feeding rate	13 m/min
Voltage	29 V
Current	257 A
Welding speed	25 cm/min
Arc energy	1.8 kJ/mm

Fig. 2 Schematic temperature-time diagram

Table 5 Short-term mechanical properties at ambient temperature and at 625 °C

Temperature (°C)	20		625	
Direction	Cross-weld	Longitudinal	Cross-weld	Longitudinal
Y.S. (MPa)		585		279
T.S. (Mpa)	668	748	327	346
El. (%)		18.8		28.8
Fracture location	HAZ		HAZ	
CVN@RT	39–45–29 J		–	

Fig. 3 Results of creep rupture tests at 625 °C
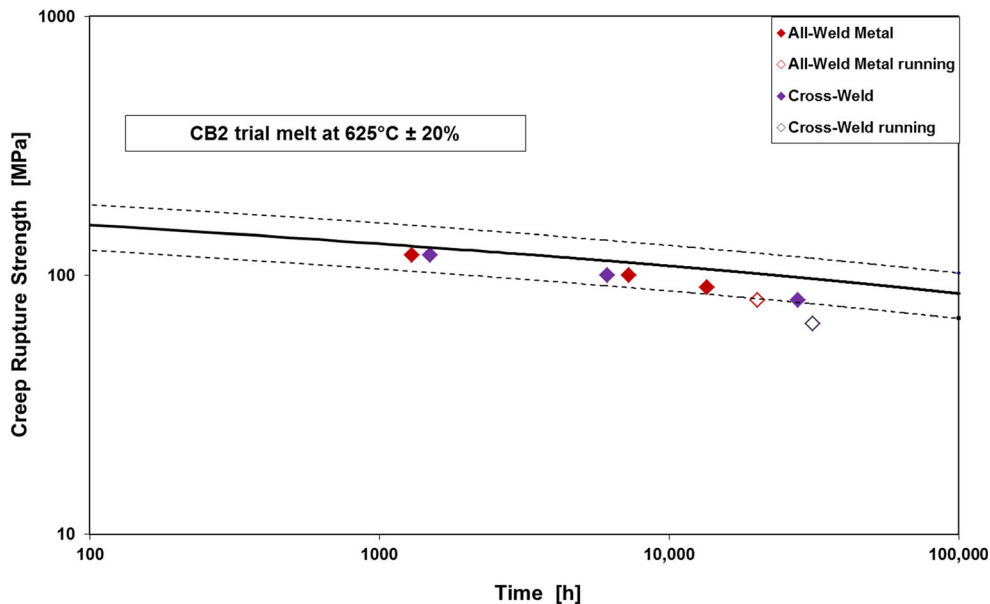
in Fig. 3. Open symbols represent still running samples. All-weld metal samples reached running times of about 1000, 7000 and 13,000 h [11]. The investigation of two cross-weld samples, which fractured after 1492 and 6118 h in the base metal and in the HAZ, respectively, has already been published [12].

Fig. 4 Macro-picture of the fractured creep sample

The cross-weld sample which is investigated in this study fractured in the HAZ after about 30,000 h with a rupture elongation of 3.3% and little reduction of area (see Fig. 4).

3.3 Simulation of microstructural evolution of the weld metal with MatCalc™

The calculation predicts the precipitation of Cr-rich carbides ($M_{23}C_6$, M_7C_3) and MX precipitates as niobium carbides (NbC) and vanadium nitrides (VN) already during the last welding cycle, which is relevant to the tempered regions of a multi-pass weld metal. M_7C_3 dissolve during PWHT and at the beginning of service, while the amount of $M_{23}C_6$ increases. Due to the long duration Laves phase, precipitation already starts during PWHT. During service $M_{23}C_6$ and Laves phase, particles are predicted to grow. Table 6 presents the calculated phase fraction and mean radius after 30,000 h of

Table 6 Prediction for the weld metal after 30,000 h in service at 625 °C

	Phase fraction (%)	Mean radius (nm)
$M_{23}C_6$	2.87	415
Laves phase	1.00	317
MX	0.22	53
BN	0.05	1010

service. A phase fraction of 1% is predicted for the Laves phase with a mean radius of about 300 nm, about 3% for $M_{23}C_6$ with a mean radius of about 400 nm and 0.2% for MX particles with a mean radius of about 50 nm as well as a small amount of large boron nitrides (BN).

3.4 Microstructure

Detailed LOM and SEM investigations of the ruptured creep sample were performed on weld metal, HAZ and base material. The results are illustrated in Fig. 5.

The formation of creep voids was investigated in unetched condition. High amounts of voids and microcracks were found in the vicinity of the fracture. In etched condition, tempered martensite was observed. Near the fracture, the grain microstructure is highly deformed. The creep voids are mainly located along the prior austenite grain boundaries. SEM investigation on base material, HAZ and weld metal operated in backscattered electrons mode revealed white particles which were assessed as Mo-rich Laves phase. Furthermore, Cr-rich carbides were also detected in all areas of the observed microstructure. Due to differences in the particle density, they appear more greyish, similar to the matrix [11].

Mo-rich Laves phase particles can easily be evaluated due to the significant white originating from the difference in the specific x-ray absorption. The statistical results of the particle size measurements are listed in Table 7.

The measured area fraction of Laves phase in the weld metal and in the HAZ is about 1% with a circle equivalent mean radius of about 160 nm. Particles up to about 600 and 500 nm, respectively, were detected. There is no significant difference between the two HAZ. In the base material, the area fraction and particle size are lightly lower.

3.5 Hardness

The hardness profile of the creep-tested sample shows a hardness range of 184 to 250 HV5 with hardness peaks in the HAZ near the fusion line and hardness drops in the HAZ with the lowest value near the rupture (see Fig. 6).

4 Discussion of results

Tensile tests and hot tensile tests indicate that the HAZ is the weakest part of the joint after welding and PWHT
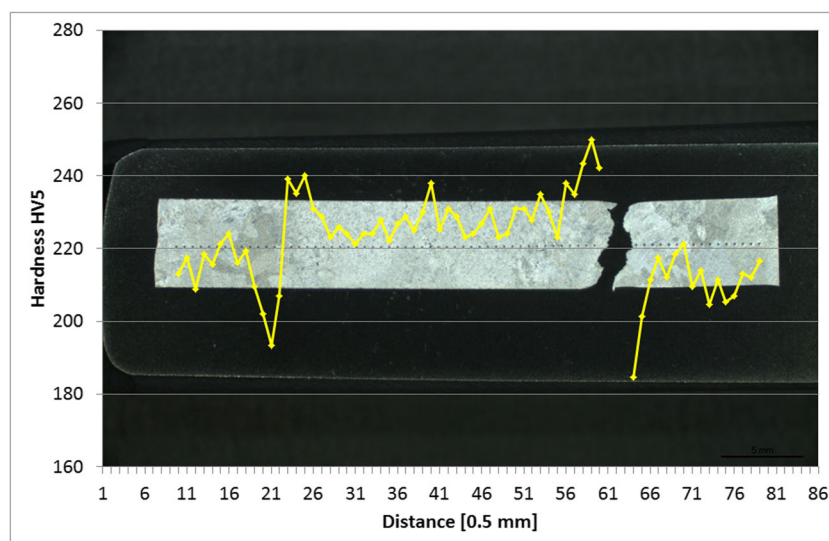
Fig. 5 Hardness profile of the creep-tested sample

**Table 7** Statistical evaluation of Laves phase particles

	Fracture	WM	HAZ	BM
Phase fraction (%)	0.95	1.00	1.03	0.82
Mean radius (nm)	169	155	162	133
Max. radius (nm)	534	614	512	479

as both cross-weld samples fractured in the HAZ and the measured strength of the longitudinal samples of the weld metal is higher than the strength of the cross-weld samples. Tensile strength and impact energy of the weld metal meet the minimum requirements at ambient temperature of 600 MPa and 27 J, respectively [13].

After 30,000 h of creep testing, the HAZ is still the weakest area. The weld metal is slightly stronger than the base material.

The evolution of Cr-rich carbides and Laves phase can be described accurately using MatCalc™ simulations. The presence of Cr-rich carbides in as-welded condition is described by Schuler et al. for a similar welded joint [14]. Generally, the presence of Laves
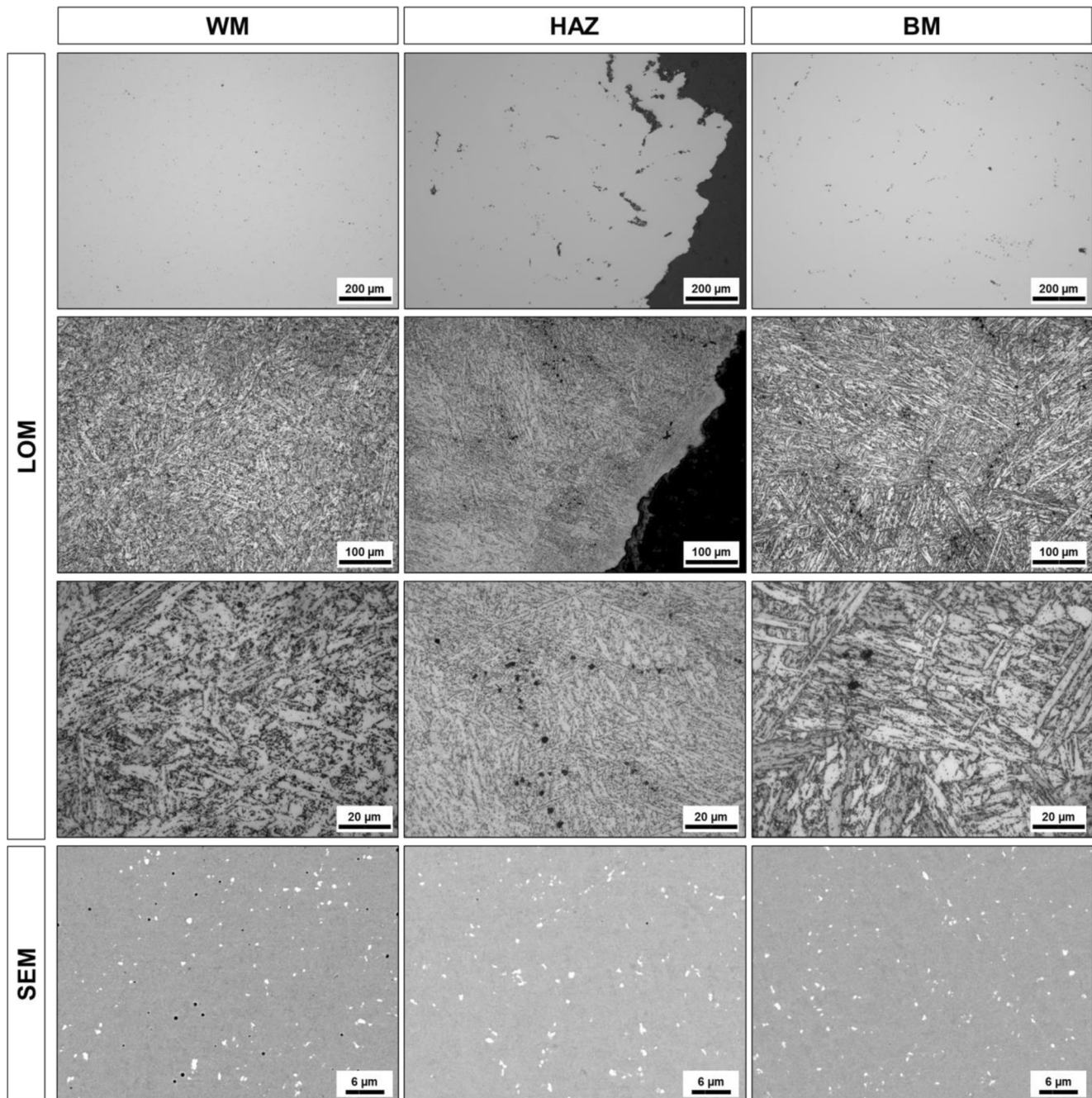
Fig. 6 LOM and SEM investigation of weld metal, HAZ and base metal

phase has been verified in various creep samples but not after PWHT so far. After 30,000 h of service or creep testing, the prediction of 1% of Laves phase corresponds to the measured value in the weld metal. However, the particle size is overestimated in the calculation. The detected Cr-rich carbides are slightly larger than the Laves phase particles. This corresponds to the prediction. Unfortunately, the grey scale of the particles is too close to the grey scale of the matrix which precludes an automated evaluation of the particles. BN was not detected in the CB2 weld metal.

More detailed microstructural investigations are necessary to verify the calculated results of $M_{23}C_6$ and MX precipitates.

5 Conclusion

A matching flux-cored wire was developed for welding cast components made of the Boron alloyed 9Cr-1.5Mo-1Co steel CB2.

Creep rupture tests at 625 °C were started several years ago to evaluate long-term properties of all-weld metal and welded joints. All ruptured samples are above the −20% line of the base material.

A cross-weld sample which ruptured after about 30,000 h was investigated by LOM, SEM and EDX.

MatCalc™ simulations were used to predict the evolution of precipitates in the weld metal during welding, PWHT and service at 625 °C and the calculated values of Laves phase precipitates after 30,000 h were compared to the experimental results.

The calculated phase fraction corresponds quite well to the measured area fraction in the creep sample. The size of the precipitates is overestimated in the calculation.

SEM investigations revealed a phase fraction of about 1% Laves phase in HAZ and weld metal and about 0.8% in the base material (Table 7). Cr-rich carbides which seem to be slightly larger than the Laves phase precipitates were detected in all areas but could not be evaluated automatically.

References

1. VGB Powertech, Facts and figures—electricity generation 2015/2016
2. Abe F (2015) Research and development of heat-resistant materials for advanced USC power plants with steam temperatures of 700 °C and above. Engineering 1:211–224
3. Kern T-U, Staubli M, Scarlin B (2002) The European efforts in material development for 650 °C USC power plants—COST522. ISIJ Int 42:1515–1519
4. Staubli M, Hanus R, Weber T, Mayer K-H, Kern T-U (2006) The European efforts in development of new high temperature casing materials—COST536. Mater Adv Power Eng Proc Part II p 855–870
5. Vanstone R, Chilton I, Jaworski P (2013) Manufacturing experience in an advanced 9%CrMoCoVNbNB alloy for ultra-supercritical steam turbine rotor forgings and castings. J Eng Gas Turbines Power 062101:1–8
6. R. Hanus (2016) Heavy steel castings for AUSC-power plants process-development and experience for materials C91, C911, CB2 and alloy 625 for heavy walled cast components; Proceedings of the 7th International Conference on Creep, Fatigue and Creep-Fatigue Interaction (CF-7), Indira Ghandi Centre for Atomic Research, Kalpokham, Tamil Nadu, India, January 19–22 (2016), p 27–34
7. Brauné E, Cerjak H, Caminada S, Jochum C, Mayr P, Pasternak J (2006) Weldability and properties of new creep resistant materials for use in ultra-supercritical coal fired power plants. Mater Adv Power Eng Proc Part II:871–891
8. Heuser H, Jochum C, Kreuzer-Zagar D (2010) Development of matching filler metals for welding CB2 and first experience; Proceedings of the 9th Liège Conference: Materials for Advanced Power Engineering 506–513
9. Baumgartner S, Posch G, Mayr P (2012) Welding advanced martensitic creep-resistant steels with boron containing filler metal. Weld World 56(7/8):2–9
10. Product Data Sheet of Böhler CB 2 Ti-FD, http://www.vabw-service.com/voestalpine
11. Baumgartner S, Pahr H, Zauchner T (2017) Creep strength of CB2 flux cored wire weld metal, Proceedings of the 4th International ECCC Creep & Fracture Conference
12. Schuler M, Baumgartner S, Schnitzer R, Enzinger N (2013) Creep investigation of CB2 joints using similar rutile CB2-flux cored wire, IIW Doc. II-1850-13. Weld World 58(6):903–913
13. Lochbichler C, Schmidtne-Kelity E, Baumgartner S (2013) Latest developments of cast materials and welding consumables for coal-fired steam turbines components/nickelbase alloy A625 and CB2 steel for the A-USC technology, Proceedings of PowerGen, Vienna
14. Schuler M, Ramskogler C, Baumgartner S, Schnitzer R, Enzinger N (2014) Simulation of Microstructure and modelling of mechanical properties of CB2 flux cored wires weld metal, Proceedings of the 10th Liege Conference: Materials for Advanced Power Engineering, edited by J. Lecomte-Beckers, O. Dedry, J. Oakey and B. Kuhn, pp. 189–198